An Analytic Magnitude and Phase fMRI Activation Model Applied to ASL

Daniel B. Rowe[1*] and Luis Hernandez-Garcia[2]

[1]Department of Biophysics, Medical College of Wisconsin, Milwaukee, Wisconsin, USA

[2]Functional MRI laboratory, University of Michigan, Ann Arbor, Michigan, USA

Synopsis

A computationally fast high tSNR magnitude and phase activation model is presented then applied to an ASL fMRI visual experiment. In fMRI, Fourier encoded k-space measurements, inverse Fourier reconstructed images, and voxel time series are complex-valued (real and imaginary or magnitude and phase). Nearly all fMRI studies derive functional activation from magnitude-only time series while discarding the phase time series. A GLM magnitude and/or phase activation model has been introduced and shown to have higher sensitivity. However, the existing method to compute magnitude and phase activation utilizes an iterative MLE algorithm while here we use a large tSNR exact solution.

Introduction

In fMRI, Fourier encoded k-space measurements are complex-valued. The inverse Fourier transform image reconstruction process produces complex-valued images. Voxel time series from a set of complex-valued images are also complex-valued (real and imaginary or magnitude and phase). Nearly all fMRI studies derive functional activation based on magnitude-only data time series [1,2]. The phase time series (half of the data values) are usually discarded. It is known that there is biological information contained within the phase time series [3,4]. Recently GLM activation models from complex-valued data have been introduced to detect changes in the magnitude and phase [2,5,6] and shown to have higher sensitivity [7]. There has been increased interest in detecting task related magnitude and phase changes in fMRI [8]. The current method to compute magnitude and phase activation [8] utilizes an iterative MLE algorithm. We present an *analytic, computationally fast* high tSNR magnitude and phase activation model then demonstrate its performance on an ASL fMRI visual stimulation experiment.

Theory

In a voxel, the observed complex-valued data at time t can be described as

$$\begin{pmatrix} y_{Rt} \\ y_{It} \end{pmatrix} = \begin{pmatrix} \rho_t \cos\theta_t \\ \rho_t \sin\theta_t \end{pmatrix} + \begin{pmatrix} \eta_{Rt} \\ \eta_{It} \end{pmatrix} \quad (1)$$

where $t=1,\ldots,n$ and the measurement errors are specified to be normally distributed with a mean of zero and variance of σ^2, $(\eta_{Rt},\eta_{It})' \sim N(0,\sigma^2 I_2)$. A transformation can be performed to convert from Cartesian coordinates for observed real and imaginary parts y_{Rt} and y_{It} to observed magnitude $m_t=(y_{Rt}^2+y_{It}^2)^{1/2}$ and phase $\varphi_t=\text{atan}(y_{It}/y_{Rt})$ to obtain $p(m_t,\varphi_t)$ [6]. The joint distribution can be written as $p(m_t,\varphi_t)=p(m_t)p(\varphi_t|m_t)$. The marginal distribution of the magnitude $p(m_t)$ is in general Ricean distributed but when the tSNR is high it is normally distributed with mean ρ_t and variance σ^2 [7]. The conditional distribution of the phase given the magnitude $p(\varphi_t|m_t)$, is von Mises distributed with mean θ_t and concentration parameter $\kappa_t = m_t\rho_t/\sigma^2$ [8]. When the tSNR is high, $p(\varphi_t|m_t)$ is normally distributed with mean θ_t and variance $1/\kappa_t$.

In addition, since the tSNR is high, one can use the approximation $\rho_t \approx m_t$. The aforementioned magnitude can be described by $\rho_t = x_t'\beta = \beta_0 + \beta_1 x_{1t} + \ldots + x_{q_1 t}\beta_{q_1}$ where x_t' is the t^{th} row of a magnitude design matrix X and β is a is a q_1 dimensional vector of magnitude regression coefficients while the phase can be described by $\theta_t = u_t'\gamma = \gamma_0 + \gamma_1 x_{1t} + \ldots + x_{q_2 t}\gamma_{q_2}$ where u_t' is the t^{th} row of a phase design matrix U and γ is a q_2 dimensional vector of phase regression coefficients [6]. With the high tSNR normality of the magnitude and phase measurements, a general linear regression model

$$\begin{pmatrix} m \\ \varphi \end{pmatrix} = \begin{pmatrix} X\beta \\ X\gamma \end{pmatrix} + \begin{pmatrix} \varepsilon_m \\ \varepsilon_\varphi \end{pmatrix} \quad (2)$$

can be written. In Eq. 2, ε_m is normally distributed with a mean of zero and covariance of $\Sigma_m=\sigma^2 I_n$ while ε_φ is normally distributed with a mean of zero and covariance of Σ_φ. The covariance matrix Σ_φ is diagonal with elements $(\sigma/m_t)^2$. Voxel-wise magnitude and phase activation can be found by testing the contrast hypotheses $H_0: C\delta=0$ vs. $H_1: C\delta\neq 0$ where $C=[C_m,0;0,C_\varphi]$, C_m and C_φ are of full row rank r_m and r_φ while $\delta=(\beta',\gamma')'$. The MLEs under H_1 are:

$$\hat{\delta} = \begin{pmatrix} (X'X)^{-1}X'm \\ (X'\Sigma_\varphi^{-1}X')^{-1}X'\Sigma_\varphi^{-1}\varphi \end{pmatrix} \quad (3)$$

and MLEs under H_0 are $\hat{\delta}_* = \Psi\hat{\delta}$ where $\Psi=[\Psi_m,0;0,\Psi_\varphi]$, for $v=m$ or φ, $\Psi_v = I-(X'X)^{-1}C_v'[C_v(X'X)^{-1}C_v']^{-1}C_v$. A likelihood ratio test can be formed and with algebra simplified to:

$$F = \frac{(C\hat{\delta})'(X_*'X_*)^{-1}(C\hat{\delta})/(r_m+r_\varphi)}{(y-X_*\hat{\delta})'(y-X_*\hat{\delta})'/(2n-r_m-r_\varphi)} \quad (4)$$

which has an F distribution with r_m+r_φ and $2n-r_m-r_\varphi$ degrees of freedom under H_0 where $X_*=[X,0;0,X]$ and $y=(m',\varphi)'$. Voxel statistics are then thresholded [9].

Experiment

ASL images were collected from a human subject using the pseudo-CASL sequence (spin-echo spiral acquisition with TR= 4000 ms, TE =15 ms, slice thickness = 7 mm, FOV = 24 cm). The labeling pulses consisted of a train of Hanning window shaped pulses (pulse width = 500 μs, pulse spacing = 290 μs, flip angle 22.5°, net gradient moment = 3×10^{-5} G/cm/s) applied for 3600 ms. The scans were collected during a visual stimulation paradigm (8 Hz flashing checkerboard: six cycles of 50 s rest – 50 s active). Five slices were prescribed encompassing the visual cortex and 150 TRs were collected. The experiment was performed using a post inversion delay of 1200 ms for arterial suppression.

Results

The complex-valued time courses were phase centered by subtracting their angular mean and spatially smoothed. A complex GLM for the unsubtracted signal was constructed with design matrix columns displayed as rows in Figure 1 [10].

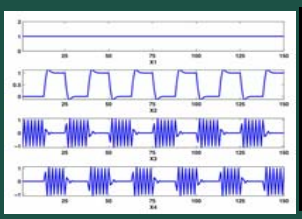

Figure 1: ASL signal design matrix.

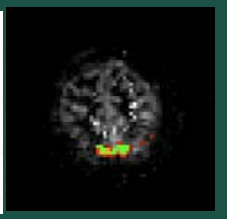

Figure 2: Activation map.

Linear and quadratic trend regressors were incorporated in order to capture trends of no interest. The linear models were estimated from Magnitude-Only, Phase-Only and Magnitude-Phase complex data. The complex data model was evaluated using MLE [6] as well as the large SNR method presented above. F statistics and their corresponding p-values were computed over the field of view. Statistical scores were extracted from a cubic ROI (3×3×3 voxels) centered on an active area on the visual cortex and compared across analysis types. In Figure 2 is the activation map (expressed as $-\log_{10}$(p-value)) overlaid on the mean perfusion map for magnitude-only analysis (blue color scale) and complex analysis ("hot" color scale) while overlapping pixels are green. All active pixels in the Magnitude-Only analysis were also active in the Magnitude-Phase analysis. Table 1 indicates the mean $-\log_{10}$(p-value) over the ROI for each analysis.

(108,75,14 mm)	MO	PO	MP
Whole Signal	1.17	0.32	1.42
PID	0.72	0.09	0.59

Table 1: Mean $-\log_{10}$(p-values) over ROIs.

Discussion

These results confirm that (1) complex analysis is beneficial for ASL FMRI data processing (2) there is more task-related phase information in ASL data when the arterial signal is preserved and (3) the new estimation method yields results that are nearly equivalent to the iterative MLE method. Simulations not shown demonstrate nearly equivalent results down to tSNRs below 5 and an order of magnitude time reduction.

References

1. Bandettini PM et al. 1993. MRM 30:161-73. 2. Rowe DB, Logan BR 2005. NIMG 24:603-6. 3. Hoogenraad FG et al. 1998. MRM 39:97-107. 4. Menon RS 2002. MRM 47:1-9. 5. Rowe DB, Logan BR 2004. NIMG 23:1078-92. 6. Rowe DB 2005. NIMG 25:1310-24. 7. Rowe DB 2005. NIMG 25:1124-32. 8. Rowe DB et al. 2007. JNSciMeth 161:331-41. 9. Logan BR, Rowe DB 2004. NIMG 22:95-108. 10. Mumford JA et al. 2006. NIMG 33:104-14.

Acknowledgements

This was supported in part by NIH EB007827, EB000215, EB004346.